OPTIMUM COMBINATION OF LOW-β CAVITIES FOR A PROTON LINAC

K. Ikeda, T. Kan, H. Yokobori, J. Hirota, Y. Iwashita*, A. Noda* and M. Inoue*
Mitsubishi Atomic Power Industries, Inc.
3-1, Minatomirai 3-chome, Nishi-ku, Yokohama-shi 220, Japan
*Nuclear Science Research Facility, Institute for Chemical Research, Kyoto Univ.
Gokasho, Uji-shi, Kyoto-fu 611, Japan

Abstract

A design study of a proton linac for multi-purpose use has been made to investigate an optimum combination of a four vane RFQ and Alvarez DTLs of 4π and 2π-mode acceleration with an operating frequency of 425 MHz. Cold model tests carried out are those of an RFQ with a field stabilization scheme, a DTL with transition from 4π to 2π-mode acceleration, and slot coupling between RFQ and DTL cavities.

Introduction

A design study of a proton linac for multi-purpose use has been made since April 1990. It is intended in this study to investigate an optimum combination of a four vane RFQ and Alvarez DTLs for 4π and 2π-mode acceleration of protons. The average beam current is aimed to be 1 mA and the operating frequency is selected to be 425 MHz because of the requirement for the neutron yield and transportability of the linac respectively.

The transition from the RFQ to the DTL of 4π-mode acceleration is set at 1 MeV so that the fabrication and adjustment of the RFQ may be facilitated. A cold model test of the RFQ was carried out to examine the effect of Resonant Loop Rings [1,2] on the mode separation and the field stabilization.

The transition from 4π to 2π-mode acceleration in the DTL is set at 2 MeV. A cold model test was carried out for making a study of the DTL with transition from 4π to 2π-mode acceleration in a single tank. The effect of double stem on the field stabilization was also investigated.

It is planned to couple the RFQ cavity with the DTL cavity, because this scheme eliminates the necessity for a separate rf power source and a drive line for the former. A simpler and more effective configuration is seemed desirable than the design of PIGMI [3] .

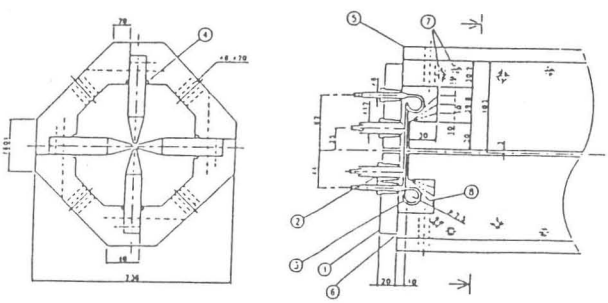

Fig. 1. Structure of the RFQ model cavity
1 End plate 2 End tuner 3 RLR
4 RF contactor 5 Cavity-wall 6 Vane
7 Cap bolt 8 Cutback-block

Mode Separation in RFQ

Structure of model cavity

The equivalent inner diameter and length of the model cavity are 154.5 and 1220.0 mm, respectively. The structure of the cavity are shown in Fig.1. The vane tip is fabricated to have a curvature of 3.00 $\pm$ 0.03 mm. Opposed to the each vane end, an end tuner is mounted on the end plates.

There are three methods to increase the mode separation and relax the tuning sensitivity; the use of Vane Coupling Rings (VCR) [4] , Resonant Loop Rings(RLR) and π mode Stabilizing Loops (PISL) [5] . Among these methods, the second scheme has been selected because the vanes are mechanically unstressed.

Resonant frequencies

An examination of the effects of the RLR scheme on the mode separation and the field stabilization is the main objective of this cold model test. The shifts of the resonant frequencies for the TE110 and TE111 modes were measured on the cavity, changing the distance between the RLR and the end plate. As expected, the resonant frequencies for the quadrupole modes are not affected by the RLRs.

The separation between the TE210 mode and TE110 modes increases from about 4.5 MHz to the value more than 10 MHz when the distance between the ring and the end plate is nearly 2.5 mm. Therefore, it can be concluded that the RLR scheme is effective on the mode separation even in case of our cavity whose ratio of the length to the free space wavelength of the operating frequency is about 1.6 [6] .

Transition from 4π to 2π-Mode in DTL

Structure of model cavity

The constant-velocity model cavity consists of 16 cells whose lengths correspond to the proton energy of about 2 MeV; 5 cells for 4π-mode acceleration, 1 cell for transition from 4π to 2π-mode acceleration and 10 cells for 2π-mode acceleration. The equivalent inner diameter and length of the cavity are 430.0 and 967.5 mm respectively. The diameter of the drift tube (DT) and bore hole are 80.0 and 10.0 mm respectively. The gap length between the DTs is determined by the SUPERFISH calculation to bring the resonant frequency at 425 MHz. The DT can be supported by either single or double stem 180° apart. The diameter of the stem is 15 mm. The half DT on each end plate can be moved to detune the end cell.

Field distribution

The on-axis electric field distribution was measured with the Bead Perturbation Method.

The average electric field (integrated electric field divided by the cell length) in the cavity with single stem was obtained: The average field in the 4π and 2π -mode cells are uniform within ± 1.6 % and ± 1.3 % respectively, except for the transition cell. There exists a difference of 5 % between the mean values of the average fields in the 4π and 2π -mode cells. The electric field distribution calculated with SUPERFISH gives the difference of 4 % which agrees satisfactorily with the measured one [7] .

Double stem and tilt sensitivity

The measured resonant frequencies are 426.43 MHz for the TM010 and 477.62 MHz for the TM011 mode in the cavity with double stem(in line). The extra stem on each DT increases the TM010 frequency by only 0.82 MHz, but increases the TM011 frequency by 28.24 MHz.

The effect of the extra stem on the field stabilization was investigated by using Tilt Sensitivity (TS) [8] : For the first measurement, decreasing the first gap lowers the TM010 mode frequency by Δf and increasing the last gap restores the frequency. The second measurement corresponds to opposite sign perturbations to the end cells, which tend to tilt the field in the opposite direction. TS is defined as:

$$TS = (E_n^+ - E_n^-)/(E_n^+ + E_n^-)\cdot\Delta f \times 100(\%) \qquad (1)$$

where E_n^+ and E_n^- are the on-axis electric field of the cell-n in the first and second measurement.

Figure 2 shows three TS measurements: The TS slope for the cavity with single stem and double stem(in line) are -38 and -12 %/MHz/m respectively. The extra stem on each DT results in an almost three fold reduction in the TS slope when the stems are installed in line each other. This higher stability is consistent with the observed large increase in the TM011 frequency. The TS behaves differently when the stems are installed cross-wise. A DTL with double stem(cross) may be advantageous in an energy region higher than 8 MeV.

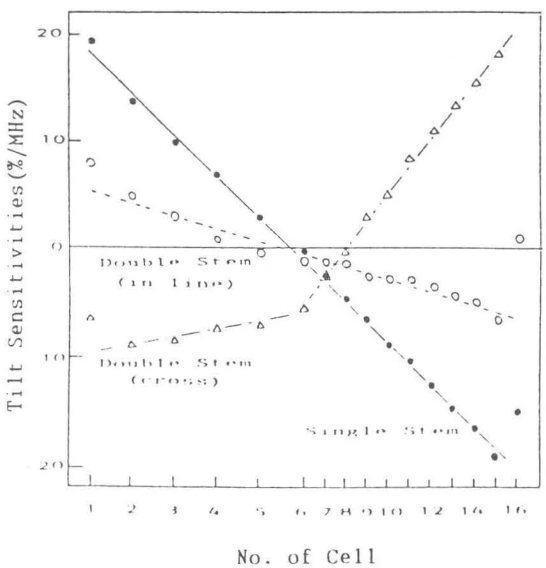

Fig. 2. Tilt sensitivities for the cavities with single and double stem

Slot Coupling between RFQ and DTL Cavities

Configuration of model cavities

The RFQ and DTL model cavity are aligned closely each other and separated by the common end plate. The DTL cavity consists of 6 cells of 4π -mode acceleration which are 68.5 mm long each and correspond to the proton energy of about 1 MeV. The equivalent inner diameter of the cavity and the diameter of the DT are 460.0 and 80.0 mm respectively. The bore radius is 5.0 mm. A side tuner and fixed tuners are provided to adjust the resonant frequency. The RFQ cavity is the existing one.

The distance, L, from the exit of the RFQ vane to the center of the first gap of the DTL should satisfy the following relation for synchronization when "half end cell" scheme of the RFQ is used:

$$L = (\Phi_{SDTL} - \Phi_{SRFQ})\beta\lambda/2\pi + n\beta\lambda/2 \quad (n = 1, 2, \cdots) \qquad (2)$$

where Φ_{SDTL} and Φ_{SRFQ} are the synchronous phase of the proton beam in the DTL and RFQ respectively.

The shape of the slot used in the test is a curved racetrack. For the nonresonant coupling, two slots with the same shape are used at the opposite positions facing to the vane ends. Figure 3 shows the slot-plates installed in the end plate and the inside of the DTL cavity. The resonant frequency of the slot itself was measured with a network analyzer. The measurement indicated that the resonant frequencies of the slots were higher than 1 GHz.

TABLE 1
Summary of the Coupling Obtained in the Test

Slot	Arc-angle (°)	Width (mm)	f_π (MHz)	f_0 (MHz)	k (%)
A-1	90	9.0	404.36	403.50	0.21
A-2	90	18.0	404.47	403.33	0.28
A-3	90	27.0	404.45	403.09	0.34
A-4	120	9.0	405.36	403.80	0.39
A-5	150	9.0	404.95	401.93	0.75
A-6	150	18.0	405.25	400.94	1.07
A-7	150	27.0	405.30	400.65	1.15

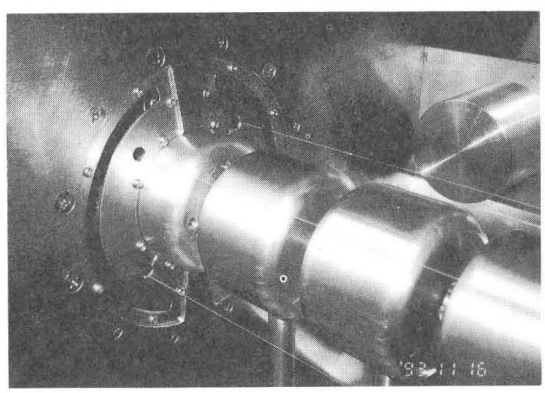

Fig. 3. The slot-plate installed in the end plate and inside of the DTL cavity

Resonant frequency and coupling constant

The coupled frequencies given in Table 1 are those measured in the following way: Firstly, the resonant frequency for the TE210 mode is measured in the RFQ cavity while the DTL cavity is detuned. Secondly, the resonant frequency for the TM010 mode in the DTL cavity is equalized to the above uncoupled RFQ (detuned DTL) frequency using the side tuner and fixed tuners while the RFQ cavity is detuned by shorting the vanes. Then, the detuning is removed and the two coupled frequencies, f_π and f_0, are measured which correspond to the π and 0-mode coupling respectively.

Using the coupling cavity theory and asuming the coupling between similar cavities, the coupling constant, k, is given as:

$$k = (f_\pi^2 - f_0^2)/(f_\pi^2 + f_0^2) \qquad (3)$$

Although k increases as the width of the slot increases, the maximum value of k is only 0.34 % when the arc-angle is limited to 90° keeping the same polarity of the magnetic flux in the end region of the RFQ cavity. If the arc-angle is expanded beyond 90°, k increases largely as seen in the table.

Field distribution

Distributions of the magnetic and electric field were measured using the Bead Perturbation Method. Preliminary measurements of the distribution of the magnetic field in the RFQ cavity indicated that the field decreased exponentially from the outlet when the 0-mode coupling was used. Since then, the π-mode coupling has been investigated.

TABLE 2
Effect of the Slot Longitudinal Position

Shift to DTL side (mm)	k (%)	Ratio of field of RFQ to DTL
0	0.75	2.26
2.0	0.71	1.74

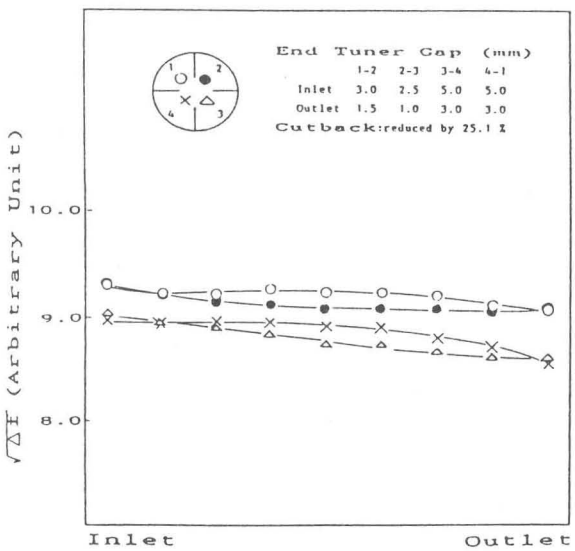

Fig. 4. Distributions of the magnetic field in the RFQ cavity with slot A-5

The measurement indicated that the magnetic field in the RFQ cavity with slot A-5 declined towards the outlet. The tilt of the field from the inlet to outlet was up to -15 %. When slot A-6 was used, the tilt increased intolerably.

The azimuthal symmetry of the magnetic field in both the cases was poor, although the end tuner gaps had been set at the optimum values for the RFQ cavity with the blind slot. Therefore, the end tuner gaps have been readjusted for the RFQ cavity with slot A-5. The result is shown in Fig. 4. These distributions are pretty good; both the azimuthal field symmetry and longitudinal field uniformity are within ±2.3 % [9] .

Longitudinal position of the slot

The effect of the longitudinal position of the slot on the excitation of the RFQ and DTL was investigated: A brass cylinder of 10 mm diameter and 15 mm length was inserted through a hole in the wall of the RFQ and DTL cavity coupled through slot A-5 and the frequency shift, Δf, was measured. Then, the longitudinal position of the slot was shifted by 2.0 mm to the DTL side and the perturbation measurement was repeated. Using the result of $\Delta f/f$, the ratio of the magnetic field on the wall of the RFQ to DTL cavity was estimated. Table 2 gives the result together with the value of k. The SUPERFISH calculations give the ratio of 2.13 which corresponds to the intervane voltage of 80 KV (1.8 times Kilpatric field criterion) in the RFQ and the average accelerating field of 3.0 MV/m in the DTL. It can be seen from the table that the appropriate ratio of the excitation of the RFQ to DTL can be obtained by shifting the longitudinal position of the slot slightly.

Conclusions

(1) The transition from the RFQ to the 4π DTL is set at 1 MeV so that the good mode separation may be achieved by using the Resonant Loop Rings.

(2) The transition from the 4π to 2π-mode acceleration in the DTL is possible by inserting the transition-cell between the 4π and 2π-cell in a single-tank structure.

(3) The extra stem on each DT improves the field uniformity.

(4) The RFQ cavity can be driven from the DTL cavity through the dual-slot provided in the common end plate.

References

[1] A. Schempp et al.: IEEE Trans. Nucl. Sci., Vol. NS-32, No. 5, p. 3252 (1983).
[2] A. Schempp et al.: PAC87 Vol. 1, p. 361 (1983).
[3] Compiled by L. D. Hansborough: LA-8880, UC-28 and UC-48 (1981).
[4] D. Howard and H. Lancaster: IEEE Trans. Nucl. Sci., Vol. NS-30, No. 2, p. 1446 (1983).
[5] A. Ueno: JHP-14, KEK Int. 90-16(1990).
[6] K. Ikeda et al.: Bull. Inst. Chem. Res. Kyoto Univ., 70, 99 (1992).
[7] K. Ikeda et al.: ibid., 71, 26 (1993).
[8] J. H. Billen: Mo3-35, 1988 Linac Conf. at CEBAF, CEBAF-Report 89-001, 125 (1989).
[9] K. Ikeda et al.: Bull. Inst. Chem. Res. Kyoto Univ., 72, 1 (1994).